Experimental Study of the Flow Field over Bottom Intake Racks

Maurizio Righetti[1] and Stefano Lanzoni[2]

Abstract: Bottom racks made by longitudinal bars are hydraulic structures widely adopted for engineering purposes. In the present paper we revisit the problem of their hydraulic design, analyzing the data obtained from a systematic series of experiments carried out in a laboratory flume. For each run we measured the diverted discharge, the water surface longitudinal profile, and using a two-dimensional backscatter laser Doppler anemometer, we measured the velocity field over the rack and in the slit between two adjacent bars. The latter measurements, in particular, allow us to obtain the along-rack distributions of the discharge coefficient to be used to determine the rate of change of the diverted discharge. We use such distributions to derive a physically based relationship relating the overall diverted discharge to the length of the rack, the void ratio, the discharge coefficient measured under static conditions, the specific head of the stream approaching the rack, and a modified Froude number. The robustness of the proposed relationship is confirmed by the comparison between the discharges calculated through the proposed relationship and those measured in an extensive series of experiments available in the literature, characterized by ranges of the relevant flow parameters much larger than those investigated in the present contribution.

DOI: 10.1061/(ASCE)0733-9429(2008)134:1(15)

CE Database subject headings: Intakes; Hydraulics; Open channel flow; Experimentation.

Introduction

Water intakes by trash racks located on the bed of streams are often adopted in relatively small mountain rivers, where steep slopes, irregular bed configuration, intense sediment transport, and rapid floods prevent the use of gated dams (Bouvard 1992). Bottom racks are also used in the construction of debris flow breakers (Mizuyama and Mizuno 1994). In some cases prismatic channels upgrading downstream and with a perforated bottom can be used as energy dissipators (Viparelli 1963). All the above classes of structures are designed to absorb as much water as possible over the minimum length. Moreover, stream bed intakes are planned to operate under extreme conditions since the entire bed load during a flood will be passing over the racks. In order to reduce as much as possible clogging phenomena longitudinal bars are commonly used. Bar clearance is chosen as a function of the granulometric characteristics of incoming sediment load and depending on the use of the diverted flow discharge. Moreover, the theoretical trash rack area (i.e., the minimum area needed to derive the designed flow) is usually increased by a suitable factor (1.5–2) to allow the water to pass through even when the rack is partially clogged by sediment jamming. Finally, the racks are inclined with respect to the bed in order to increase the unclogging efficiency.

Due to their engineering relevance, the problem of correctly designing the minimum bottom area needed to convey the prescribed flow discharge has attracted the attention of several researchers (Garot 1939; Bouvard 1953; Kuntzmann and Bouvard 1954; Orth et al. 1954; Noseda 1955 1956a,b; Mostkow 1957; Brunella et al. 2003) who investigated the problem both theoretically and experimentally.

Theoretical analyses assume that the flow field above the rack can be treated as one-dimensional and, moreover, gradually varying such that the hydrostatic pressure distribution holds on each cross section. In practice, however, the flow field is characterized by streamline curvature and, hence, by a departure from hydrostatic pressure distribution (Mostkow 1957; Venkataraman et al. 1979; Righetti et al. 2000). The hydraulic behavior of bottom racks is also strongly influenced by the particular arrangement of bars forming the rack (e.g., Bouvard 1953; Motskow 1957). In the case of longitudinal bars, in fact, the diverted discharge is expressed as a function of the local value of the flow energy while in the case of transversal bars or circular perforations the outflow discharge is related to the local flow depth. In the present contribution we focus our attention on racks made with longitudinal bars that, as discussed above, are extensively used in damless intakes.

Another assumption usually employed is that energy dissipation along the rack is either negligibly small (Bouvard 1953; Motskow 1957) or balances bottom slope (Garot 1939; Noseda 1955). The former hypothesis is indeed valid for racks formed by longitudinal bars, even though the experiments carried out by Venkataraman et al. (1979) indicate that energy dissipation tends to increase with Froude number and split opening. The measurements of free surface velocities carried out by Brunella et al. (2003) confirm that dissipative effects are negligible except towards the end of the rack. Assuming that the flow energy per unit

[1]Assistant Professor, Dipt. di Ingegneria Civile e Ambientale, Univ. di Trento, Via Mesiano 77, 38100 Trento, Italy. E-mail: maurizio.righetti@ing.unitn.it

[2]Associate Professor, Dipt. di Ingegneria Idraulica, Marittima Ambientale e Geotecnica, Univ. of Padua, via Loredan 20, I-35131 Padova, Italy. E-mail: lanzo@idra.unipd.it

Note. Discussion open until June 1, 2008. Separate discussions must be submitted for individual papers. To extend the closing date by one month, a written request must be filed with the ASCE Managing Editor. The manuscript for this paper was submitted for review and possible publication on January 13, 2006; approved on July 3, 2007. This paper is part of the ***Journal of Hydraulic Engineering***, Vol. 134, No. 1, January 1, 2008. ©ASCE, ISSN 0733-9429/2008/1-15–22/$25.00.

Table 1. Summary of Relationship Proposed in the Literature to Estimate the Flow Discharge through a Bottom Rack with Longitudinal Bars

Reference	dq/dx	C_q
Garot (1939)	$C_q\omega\sqrt{2gD}$	constant[a]
De Marchi (1947)	$C_q\omega\sqrt{2gH_0}$	constant [a]
Bouvard (1953)	$C_{q0}\omega\sqrt{2gD(x)\cos\theta}$	constant [a]
Noseda (1956b)	$C_q\omega\sqrt{2gD(x)}$	$\propto[D(x)/B]^{-0.13}$
Mostkow (1957)	$C_q\omega\sqrt{2gH_0}$	constant [b]
Brunella et al. (2003)	$C_{q0}\omega\sqrt{2gD(x)\cos\theta}$	constant[c]

Note: dq/dx=flow discharge through the grid per unit width and unit length; C_q=discharge coefficient; C_q=discharge coefficient measured under static conditions; H_0=specific flow head of the flow approaching the rack; ω=void ratio; $D(x)$=local flow depth; θ=angle which the rack axis forms with the horizontal; and B=bar clearance.

[a]The values of the constant is not specified.

[b]On the basis of the experiments carried out by Orth et al. (1954), C_q is suggested to vary in the range of 0.514–0.609 for horizontal racks and 0.441–0.519 for racks inclined at 1/5 slope.

[c]The values of the discharge coefficient measured under static conditions indicate a slight dependence on the orifice Reynolds number and a stronger dependence on rack porosity. In particular, for small enough bar clearance C_{q0} can attain values greater that one owing to the Coanda effect.

weight $E=z_b+D+U^2/2g$ is everywhere constant (here, z_b denotes bottom elevation above a horizontal datum, g=gravitational constant while D and U=cross-sectionally averaged flow depth and velocity, respectively), a first-order, sixth-degree ordinary differential equation can then be obtained, which allows evaluating the flow discharge at any cross section (Bouvard 1953; Kuntzmann and Bouvard 1954). On the other hand, the hypothesis that energy dissipation equals bottom slope implies that the specific flow head $H=E-z_b$ keeps constant along the rack. Following the approach developed by De Marchi (1947) to study the surface profiles in a gradually steady flow with progressively decreasing discharge, Noseda (1955) was then able to obtain an analytic solution yielding the length of the racks as a function of either the flow depths or the flow discharges at the beginning and at the end of the rack itself. A generalization of Noseda's solution has been proposed by Brunella et al. (2003), including the effect of rack inclination with respect to the channel bed.

The development of modern computers and the application of computational techniques have made it possible to relax the above assumptions of constant E or H, solving numerically the differential equation governing the motion in prismatic channels with decreasing discharge (see Henderson 1966; Yen and Wenzel 1970). Nevertheless, the choice of the relationship specifying the outflowing discharge still deserves some attention.

Generally, the rate of change of the diverted discharge per unit width is given by the relationship

$$\frac{dq}{dx} = C_q\omega\sqrt{2gY} \tag{1}$$

where dq=discharge per unit width diverted along a piece of grid of length dx; ω=void ratio, i.e., the ratio of the openings area to the total area; Y=suitable value of the hydraulic head, and C_q=discharge coefficient. The latter coefficient depends on the hydraulic characteristics of the approaching flow, the geometry of the rack (e.g., length, slope, orientation), and of the bars forming the rack (form, size, spacing). Obviously, the values assumed by C_q are strictly linked to the definition of the hydraulic head. As reported in Table 1, different approaches have been proposed in the literature to evaluate C_q and Y. Only Noseda (1956b), however, accounts for the variability of the discharge coefficient along the rack, assuming that C_q is proportional to the ratio of the local flow depth to bar clearance. As a result C_q can vary in the quite wide range 0.7–1.0.

The review of the existing literature then clearly shows that an univocal definition of the relevant hydraulic head to be used in Eq. (1) does not exist and that the parametrization of C_q needs to be carefully addressed. Indeed, none of the proposed approaches is derived on the basis of a dimensional analysis methodology nor are they verified through direct measurements of the flow field above and in between the rack bars. These measurements could be particularly effective for an exhaustive comprehension of the phenomenon and a correct parametrization of the discharge coefficient.

The present contribution thus aims at investigating experimentally the validity of the simplifying assumptions usually adopted in the study of the flow over bottom racks with longitudinal bars, at identifying the relevant dimensionless parameters, and at developing a physically based relationship allowing the correct design of bottom racks. To this end it is worthwhile to note that the hydraulic configuration given by a bottom rack of finite length L can be regarded as an intermediate case between a bottom slit (as L tends to zero) and a free overfall (as L tends to infinity). In both cases the characteristics of the flow field (i.e., the diverted flow in the first case, the free overfall geometry in the latter) are found to depend on the depth and on the Froude number of the incoming flow (Venkataraman et al. 1979; Nasser et al. 1980; Hager 1983; Marchi 1993; Ferro 1992; Khan and Steffler 1996; Davis et al. 1999; Oliveto et al. 1997). The rest of the paper is organized as follows. The second section describes the experimental apparatus and summarizes the various tests. The third section is devoted to the discussion of the experimental results. Finally, we report some concluding remarks.

Experimental Apparatus

The tests were carried out in a laboratory flume 12 m long and 0.25 m wide, with sidewalls consisting of a steel frame with glass windows. The entire flume can be tilted up to a 5% slope. A rack of length L=0.45 m and with a void ratio ω=0.2 was located on the channel bottom 6 m downstream from the inlet section of the flume, as it is shown in Fig. 1. Both the rack and the bottom were made of perspex in order to allow the optical access also in the slots between the bars forming the rack. A two-dimensional (2D) backscatter laser Doppler anemometer (LDA) was used to measure the velocity field over the racks and in the slit between two adjacent bars.

The shape of the longitudinal bars forming the rack, whose characteristics are shown in Fig. 1, has been chosen to prevent, as much as possible, flow separation. Such a choice optimizes the optical access of the LDA system. Moreover, the use of round-ended bars, usually with a tapered cross section, is highly recommended in designing stream bed intakes in order to ensure a better efficiency (Orth et al. 1954) and to prevent sediment from jamming (Bouvard 1992). The discharge coefficient C_{q0} characterizing the adopted rack, measured under static conditions, was found to vary in the range of 0.95–1. Note that as recently pointed out by the measurements made by Brunella et al. (2003), C_{q0} can also attain values higher than one as a consequence of the Coanda

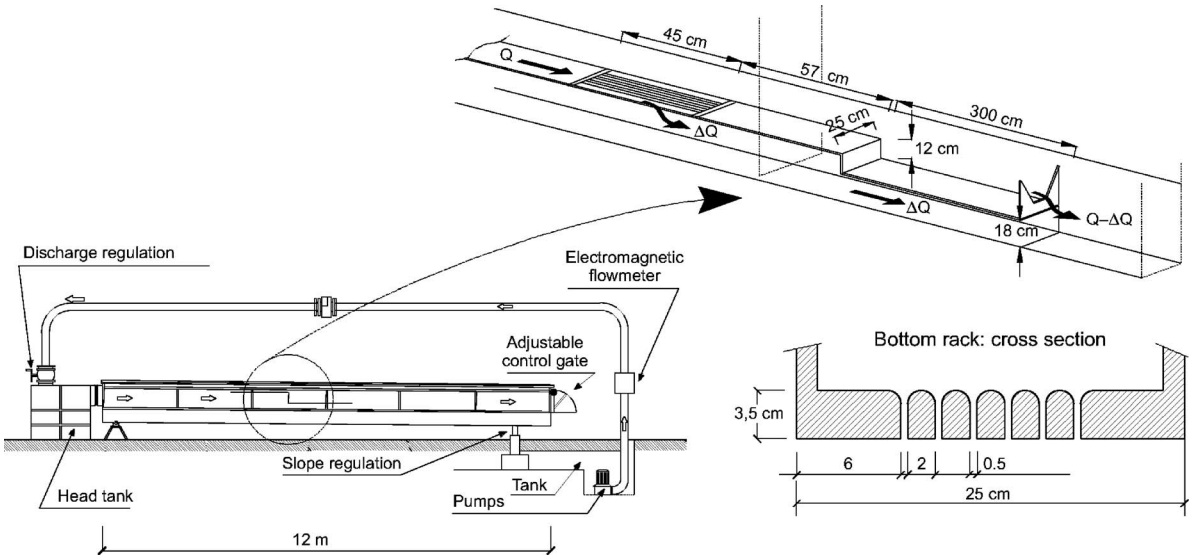

Fig. 1. Sketch of the experimental apparatus and geometrical characteristics of the adopted rack

effect arising when bar clearance is small enough.

The water discharge was supplied by a constant head tank located upstream of the inlet section of the flume. Both the water diverted by the grid and the water flowing downstream were collected in a tank located below the flume and pumped through a recirculation pipe to the head tank. The total water discharge supplied to the flume was measured using a magnetic flow meter located in the recirculation pipe, while the water flowing downstream of the grid was measured through a weir located at the end section of the flume.

The water surface was measured automatically along the axis of the flume by a profiler mounted on a carriage moving along two rails parallel to the bottom of the flume. Indeed, a preliminary series of tests carried out in the same flume by Righetti et al. (2000) indicate that, at a given section, the departure from cross-sectionally averaged flow depth keeps usually small enough to be neglected for the practical design of a rack. Even though transverse curvatures of the free surface tend to increase with decreasing flow depth, longitudinal water surface profiles can be taken approximately identical both on the bars and on the openings above the largest part of the rack, in accordance with Noseda's (1955) observations.

A laser Doppler anemometer was used to measure the velocity components along several verticals located either over the bar or the openings and in the slit between two adjacent bars. Moreover, the trajectories of the fluid particles along the flow field were reconstructed by using a particle tracking velocimetry (PTV) technique (Righetti et al. 2000). To this end a suitable amount of tracing particles was released in the fluid and a longitudinal sheet of light was generated over the grid by using a beam of laser light passing through a system of optical lenses. The portion of flow field lighted by the sheet of light was then filmed through a fast frame rate video camera and the trajectories of the tracking particles were finally detected.

The hydraulic characteristics of the various experimental runs are reported in Table 1 where: D_0, Q_0, and F_{r0}=flow depth, the water discharge, and Froude number of the approaching uniform flow, respectively; i_b=bottom slope of the flume; Q_f=water discharge flowing downstream of the grid; and ΔQ=water discharge diverted through the grid. Basically, two series of tests have been carried out fixing either (1) the flow depth or (2) the Froude number of the incoming stream. In particular, we focused our attention on the case, typically, encountered in practical applications on mountain streams, of supercritical approaching flow.

Discussion of Experimental Results

General Features

Before discussing in detail how the present results can be used to obtain a physically based estimate of the discharge coefficient, it may be worthwhile to briefly describe some general features emerging from both present tests and a series of preliminary runs carried out in the same flume by Righetti et al. (2000). A comprehensive view of the longitudinal water profile measured along the flume is shown in Fig. 2 for all the experiments listed in Table 2. Owing to the supercritical character of the approaching flow, the depth decreases along most of the grid. In analogy with the case of a free overfall (Hager 1983; Marchi 1993), the effect of the grid extends slightly upstream of its initial section as a consequence of streamline curvature. On the other hand, the stagnation point at the downstream end of the rack induces a local increase of the flow depth.

Curvature effects are even more evident in the streamline pattern reconstructed from PTV analysis and reported in Fig. 3. In particular, the streamlines are deflected downward along most of

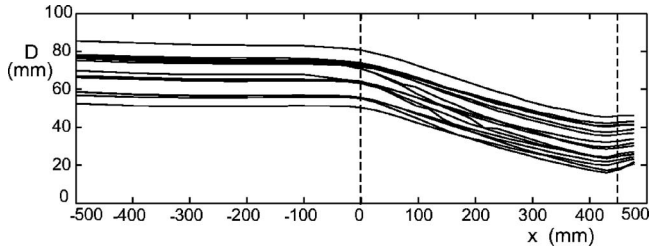

Fig. 2. Water depth profiles measured along the axis of the flume for all the experiments listed in Table 2; vertical lines denote the beginning and end of the bottom rack

Table 2. Summary of Hydraulic Experimental Conditions

Run	D_0 (cm)	Q_0 (l/s)	F_{r0}	i_b %	Q_f (l/s)	ΔQ (l/s)
1	9.0	37.3	1.77	2.5	20.1	17.2
2	8.0	36.3	2.05	4.0	20.2	16.1
3	8.0	35.0	1.97	3.5	19.0	16.0
4	8.0	33.8	1.90	3.0	17.9	15.9
5	8.0	31.7	1.80	2.5	16.4	15.3
6	8.0	29.5	1.65	2.0	14.5	15.0
7	8.0	24.0	1.35	1.0	9.8	14.2
8	8.0	21.2	1.20	0.7	7.6	13.6
9	7.0	28.9	2.00	3.5	14.4	14.5
10	7.0	26.2	1.80	2.5	12.3	14.1
11	7.0	22.2	1.50	1.5	8.3	13.9
12	7.0	18.6	1.30	0.7	5.1	13.5
13	6.0	23.2	2.00	3.5	10.0	13.2
14	6.0	21.0	1.80	2.5	8.1	12.9
15	6.0	17.8	1.50	1.5	4.7	13.1
16	5.5	20.4	2.02	3.5	7.9	12.5

Note: D_0=flow depth of the approaching flow; Q_0=discharge of the approaching flow; F_{r0}=Froude number of the approaching flow; i_b=flume slope; Q=discharge downstream the grid; and ΔQ=discharge diverted through the rack.

the grid; on the contrary, their curvature is directed upward in the final reach of the grid, as a consequence of the rear stagnation point. Due to the curvature effects, at the beginning of the rack the pressure distribution along the direction normal to the flow results, in general, lower than the value prescribed by the hydrostatic distribution, while it tends to exceed the hydrostatic value when approaching the end of the rack (Motskow 1957; Righetti et al. 2000).

The overall picture emerging from Fig. 3 is confirmed by the plots of Fig. 4, reporting the distribution of the velocity vectors measured in a vertical plane passing through a slit between two adjacent bars, for two runs characterized by the same approaching flow depth but with different Froude numbers. The velocities were measured above the rack and in-between the two adjacent bars, 0.03 m below the bottom of the flume. It clearly appears that the vertical component of the velocities within the slit is higher than in the flow field above the grid and tends to have a magnitude comparable with the horizontal component. Moreover, the vertical component decreases moving downstream along the slit, thus implying that the diverted discharge tends to decrease. Indeed, the magnitude of the downward rotation experienced by the velocity vector near the bottom and in the slit decreases progressively as one moves towards the end of the grid and, for a given value of the approaching flow depth, as the Froude number increases. Figs. 3 and 4 then suggest that the diverted discharge per unit length decreases along x and the total diverted discharge ΔQ decreases with F_{r0}. Moreover, localized end effects induced by

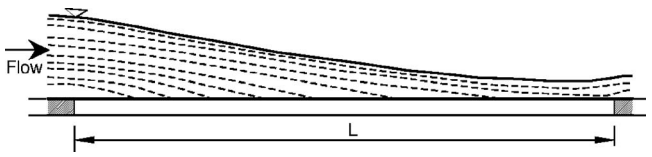

Fig. 3. Typical example of average streamlines observed in Run 10, reconstructed through PTV technique

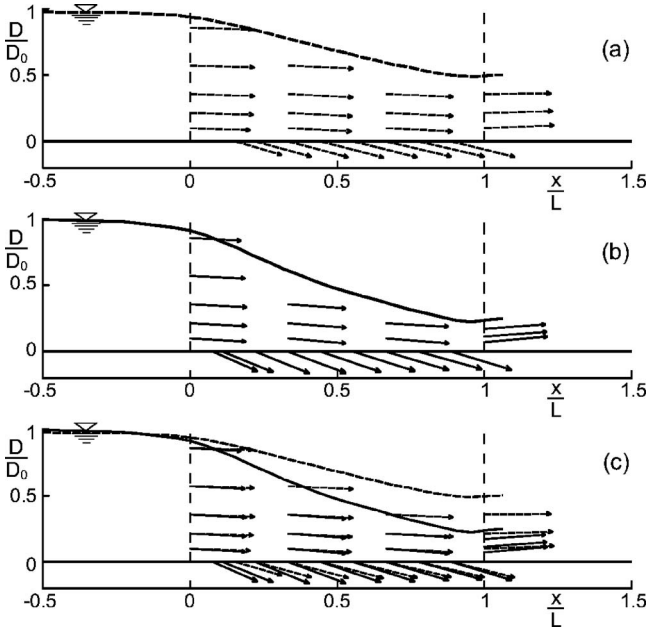

Fig. 4. Distribution of the velocity vector in a vertical plane passing through the axis of the slit between two adjacent bars, measured during (a) Run 2 (F_{r0}=2.05, D_0=8 cm) and (b) Run 8 (F_{r0}=1.20, D_0=8 cm); (c) comparison between the two velocity patterns: Run 2, thick line and Run 8, thin line

the curvature of the streamline detaching from the upstream edge of the rack and by the rear stagnation point could lead to a reduction of the diverted discharge with respect to theoretical predictions.

Finally, Fig. 5 reports the transverse distribution of the vertical component U_y of the velocity measured in the slit between two adjacent racks at three different locations along the grid (i.e.,

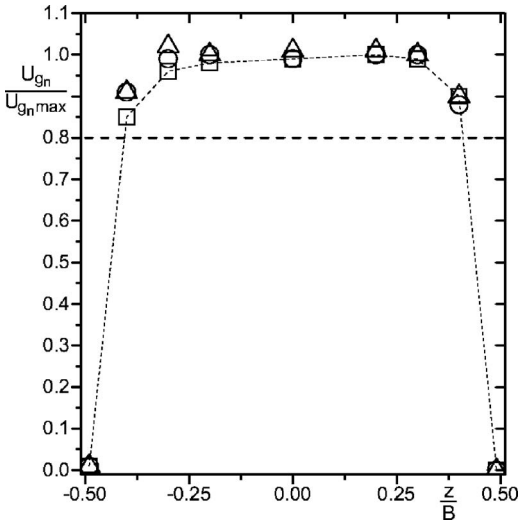

Fig. 5. Typical transverse distribution of the vertical component of the velocity, U_y, measured in the slit between two adjacent bars 0.03 m below the bottom of the flume at: (□) x/L=1/6; (○) x/L=1/2; and (△) x/L=5/6. Data refer to Run 10. $U_{y\,\max}$ denotes the maximum value of the vertical component of the velocity; z=transverse coordinate; and B=bar clearance. Dashed horizontal line indicates the cross-sectional average of U_{gn} scaled by $U_{gn\,\max}$.

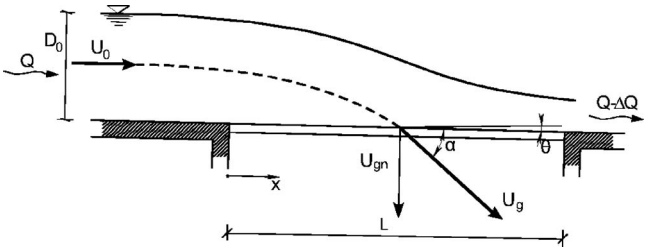

Fig. 6. Sketch of the flow field and notations

$x/L=1/6$, 1/2, 5/6). The various profiles, scaled by the maximum speed, appear to be self-similar, the average velocity within the slit being related to the maximum velocity by a factor $\alpha_u=0.8$. This coefficient will be used later on to obtain the correct value of the discharge per unit length diverted through a slit.

Discharge Coefficient

The main dimensionless parameters affecting the steady flow taking place within the slit between two adjacent bars may be identified through a dimensional analysis of the phenomenon. Neglecting the effects related to surface tension and fluid compressibility, the physical law governing the outflow at a generic distance x from the beginning of the rack takes the form

$$\mathcal{F}\left(\rho, g, U_0, H_0, J, x, \frac{dq}{dx}, \theta, \text{form}\right) = 0 \tag{2}$$

where ρ=water density; g=gravitational constant; U_0 and H_0=velocity and the specific head of the stream approaching the rack, respectively; J=energy dissipated per unit weight of fluid and unit length; dq/dx=discharge diverted per unit grid length; θ=angle that the rack axis forms with the horizontal, and form indicates the dependence on the geometric characteristics of the bars forming the rack (e.g., void ratio, shape of the cross section of the bars). Choosing H_0, U_0, and ρ as fundamental variables, and applying the Buckingham's Π theorem yields

$$\frac{dq/dx}{\sqrt{2gH_0}} = \Phi_1\left(\frac{x}{H_0}, \mathsf{F}_{H_0}, J, \theta, \text{form}\right) \tag{3}$$

where $\mathsf{F}_{H_0}=U_0/\sqrt{gH_0}$=modified Froude number $(=\mathsf{F}_{r0}/\sqrt{1+\mathsf{F}_{r0}^2/2})$ build up with the energy head H_0 instead of the depth D_0 of the approaching flow.

The energy balance along a generic streamline implies that

$$H_0 = \frac{U^2}{2g} + \Delta E - \Delta z \tag{4}$$

where ΔE $(=Jx)$ and Δz $(=x\sin\theta)$=energy loss per unit weight of fluid and the difference in height experienced along the streamline, respectively. With the notations reported in Fig. 6, it then follows that:

$$U_{gn} = U_g \sin\alpha = \sin\alpha\sqrt{2gH_0\left(1+\frac{\Delta z-\Delta E}{H_0}\right)} \tag{5}$$

where α=angle in which the velocity vector just below the slit forms with the direction of the channel axis and U_{gn} is the component normal to the grid of the velocity vector $\vec{U}_g$ at the slit exit. The experimental studies carried out by Noseda (1955), Mostkow (1957), Venkataraman et al. (1979) for longitudinal bars suggest that

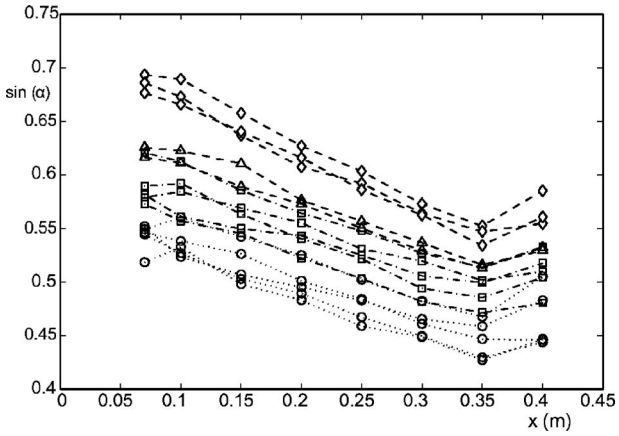

Fig. 7. Distribution of $\sin\alpha$ in the slit between two adjacent bars 0.03 m below the bottom of the flume for all the experiments listed in Table 2. (○) Runs with F_{ro} in the range of 1.30–1.47; (△), runs with F_{ro} in the range of 1.70–1.82; (□) runs with F_{ro} in the range of 1.98–2.04; and (◦) runs with F_{ro} in the range of 2.21–2.33.

$$\frac{\Delta z-\Delta E}{H_0} \ll 1 \tag{6}$$

especially in the case of racks inclined as the channel bed, for which the component of the weight parallel to the bottom tends to balance energy loss. It is thus reasonable to approximate the value taken by U_{gn} as

$$U_{gn} \simeq \sin\alpha\sqrt{2gH_0} \tag{7}$$

The discharge diverted, per unit width and unit length, by the bottom rack intake, dq/dx, then results

$$\frac{dq}{dx} = \omega U_{gn} = \omega\sin\alpha\sqrt{2gH_0} \tag{8}$$

Substituting this relationship into Eq. (1) (where H_0 is chosen as the hydraulic head) and Eq. (3), we finally obtain

$$C_q = \sin\alpha = \Phi\left(\frac{x}{H_0}, F_{H_0}, \text{form}\right) \tag{9}$$

with $\Phi=\Phi_1/\omega$.

Note that the dependence of Φ on J and θ is likely to be negligibly small, owing to condition (6). Moreover, it is worthwhile to remark that: (1) the choice of H_0 as the hydraulic head is consistent with the experimental evidence that the velocity at a given point x within the slit exit can be evaluated by the energy balance along the streamline passing through the point itself; and (2) the discharge coefficient takes on a geometrical meaning, because it approximately coincides with the sine of the angle formed by the horizontal and the direction of the velocity at the slit exit.

The dependence of C_q on the dimensionless parameters x/H_0 and F_{H_0} emerging from dimensional analysis can be investigated using the present experimental data and recalling the two constraints which have to be satisfied as the Froude number of the approaching current tends either to zero or to a value much higher than 1. In the first case, in fact, C_q tends to the constant value C_{q0}, measured under static conditions; in the latter, the diverted discharge is expected to asymptotically vanish. Fig. 7 reports an overall view of the distribution along x of $\sin\alpha$ (i.e., C_q), obtained from the measurements of the velocity vector in a slit

between two adjacent bars, 0.03 m below the bottom of the flume (i.e., nearly outside the slit). The experimental values, falling in the range of 0.4–0.7 are significantly lower than the values measured under static conditions, falling in the interval of 0.95–1. As already suggested by the velocity patterns reported in Fig. 4, it clearly appears that $\sin\alpha$ decreases almost linearly along the rack except towards its end, where the presence of a stagnation point invariably induces a local increase. Neglecting such an increase, we observe that the various curves tend to shift down almost parallel as F_{r0} increases. The decrease experienced by $\sin\alpha$ in the downstream direction is associated to two dimensional characters of the flow field which are not explicitly considered in the unidimensional treatment of the problem leading to define a discharge coefficient. As shown in Figs. 3 and 4, in fact, the higher values of $\sin\alpha$, attained in the upstream portion of the grid, are associated to the streamlines which, at the inlet section, are located closer to the bed and, hence, characterized by a lower value of the velocity speed. On the other hand the faster streamlines that, at the inlet section, are located closer to the water surface, experience a smaller deflection by gravity effects, thus leading to smaller values of $\sin\alpha$ in the downstream portion of the grid.

A relationship ensuring an almost linear dependence of C_q on the longitudinal coordinate x and satisfying the above constraints can be cast in the form

$$C_q = C_{q0}\left(a\frac{x}{H_0}F_{H_0}+1\right)\tanh[b_0(\sqrt{2}-F_{H_0})^{b_1}] \qquad (10)$$

Indeed, the function $\tanh[b_0(\sqrt{2}-F_{H_0})^{b_1}]$ is able to describe the nonlinear increase of the discharge coefficient with F_{H_0}, emerging from the analysis of the observed values of the discharge coefficient. Also, the function tends rapidly to 1 for relatively high values of b_0, thus allowing to recover the static value Cq_0 as the parameter F_{H_0} tends to zero. Finally, the function tends to zero as F_{H_0} attains its maximum value ($=\sqrt{2}$).

The coefficient a appearing in Eq. (10) has been estimated by fitting with a straight line, in terms of the independent variable $F_{H_0}\,x/H_0$, the values of C_q measured along the rack for each run and taking the average value of the ratios of the angular coefficient to the intercept. The coefficients b_0 and b_1 appearing in the hyperbolic tangent were obtained by minimizing the sum of the errors between the computed and measured total discharge diverted through the grid. A genetic algorithm procedure has been used to carry out such a minimization. Following this procedure, the estimated values are: $a=-0.1056$ and $b_0=1.5$, $b_1=0.6093$.

In order to test the validity of the functional relationships (10) we have compared the total diverted discharges calculated using this relationship with those measured by Noseda (1956a,b). It is worthwhile to remark that such a data set has been obtained: (1) using racks made by longitudinal bars with sharp edges, thus enhancing flow separation; in particular, the discharge coefficient under static conditions, was found to be nearly 0.72 for water depths above the rack greater than 4 cm; (2) inclining each investigated rack at a slope of 0, 10, and 20% with respect to the channel bed; (3) varying the void ratio ω in the range of 0.16–0.28; (4) varying the Froude number F_{r0} in the interval of 0.2–3, much wider than the one (1.3–2.3) characterizing present experiments. Therefore, the validation of Eq. (10) through the independent data set provided by Noseda's experiments turns out to be a particularly severe test, owing to the significant differences with respect to present tests.

For a given experiment, the diverted discharge ΔQ is thus estimated through the following relationship, obtained by integrating Eq. (8) in which Eq. (10) has been included for the evaluation of Cq:

$$\Delta Q = C_{q0}\omega WL\sqrt{2gH_0}\left(\frac{a}{2}\frac{L}{H_0}F_{H_0}+1\right)\tanh[b_0(\sqrt{2}-F_{H_0})^{b_1}] \qquad (11)$$

where W= channel width; for C_{q0} the experimental values measured under static conditions have been used. The comparison between computed and measured data is reported in Fig. 8. The agreement is surprisingly good in spite of the differences between the two independent data sets used to calibrate (present data) and to validate (Noseda's data) the proposed relationship. Indeed, the differences between predicted and measured discharges differs not more than 15%, thus supporting the reliability of relationship (10).

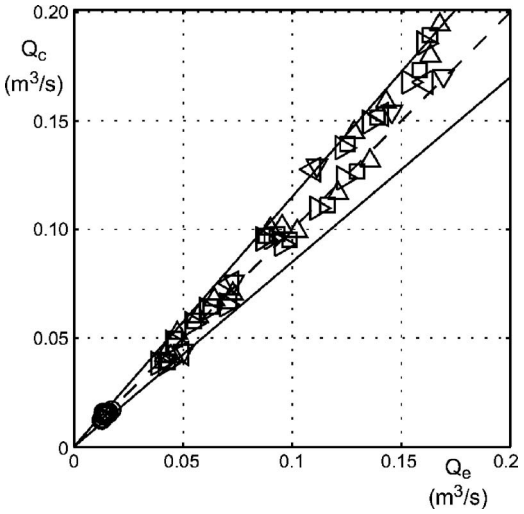

Fig. 8. Comparison between measured and estimated diverted discharges in bottom racks with longitudinal bars. Dashed line represents perfect agreement. Data falling between solid lines are such that $|\Delta Q_c-\Delta Q_e|<15\%\Delta Q_e$. (○) Present experiments; Noseda experiments: (△) rack parallel to the bed, $F_{r0}<1$; (□), rack with a 10% slope with respect to the bed, $F_{r0}<1$; (▷), rack with a 20% slope with respect to the bed, $F_{r0}<1$; (∇), rack parallel to the bed, $F_{r0}>1$; and (◁), rack with a 20% slope with respect to the bed, $F_{r0}>1$.

Conclusions

Bottom racks with longitudinal bars are widely adopted in damless intakes on small mountain rivers to divert water for hydroelectric purposes, retaining, at the same time, sediment and solid matter larger than bar clearance. We have revisited the problem of their hydraulic design analyzing the data obtained from a systematic series of experiments in a laboratory flume. For each run we measured the diverted discharge, the water surface longitudinal profile and, using a 2D backscatter laser Doppler anemometer, the velocity field over the rack and in the slit between two adjacent bars. The latter measurements allowed us to obtain the spatial distribution along the rack of the angle α that the velocity vector within the slits forms with the direction of the channel axis. The energy balance along a generic streamline indicates that $\sin\alpha$ tends to coincide with the discharge coefficient C_q provided that:

(1) the specific head of the stream approaching the rack, H_0, is chosen as hydraulic head in relationship (1) giving the diverted discharge and (2) the energy loss for unit weight of fluid almost balances the difference in height experienced along a given streamline. The longitudinal distributions of $\sin\alpha$ measured for the various experimental runs have thus been used to derive a relationship relating the discharge coefficient to the longitudinal coordinate, x, scaled by H_0, and a modified Froude number, F_{H_0}, built up with the mean velocity and the specific head of the flow approaching the rack. The functional form of the relationship accounts for the observational evidence that $\sin\alpha$ decreases almost linearly along the rack, and for the requirement that C_q must either tend to its static value C_{q0} or to zero, as the Froude number of the approaching flow tends to vanish or to attain values much larger that one, respectively. The proposed relationship appears to provide a robust estimate of the overall discharge diverted by the rack. Indeed, the comparison with an independent and wide data set, obtained by Noseda (1955, 1956a,b) for ranges of the relevant flow parameters much larger than those investigated in the present contribution, turns out to be pretty good. In particular, the diverted discharges estimated by Eq. (11) differ by no more than 15% from the observed values despite: (1) the different shapes of the rack bars; (2) the rack inclination with respect the channel bed; and (3) the subcritical, supercritical character of the flow upstream the rack.

Acknowledgments

The writers were grateful to Fabio Sartori and Alessandra Tambara of University of Trento (Italy), Department of Civil and Environmental Engineering for the profitable cooperation during the laboratory measurements.

Notation

The following symbols are used in this paper:

- a, b_0, b_1 = empirical coefficients;
- B = bar clearance between two adjacent bars;
- C_q = discharge coefficient;
- C_{q0} = discharge coefficient under static conditions;
- D = local value of the mean flow depth along the channel;
- D_0 = mean depth of the flow approaching the grid;
- dq = discharge diverted per unit grid length and per unit channel width;
- E = flow energy;
- F_{r0} = Froude number of the flow approaching the grid;
- F_{H_0} = modified Froude number, defined as $\mathsf{F}_{H_0}=U_0/\sqrt{gH_0}$;
- g = gravitational constant;
- H = specific flow head;
- H_0 = specific flow head of the flow approaching the grid;
- i_b = bottom slope of the flume;
- L = rack length;
- Q_0 = water discharge of the flow approaching the rack;
- Q_f = water discharge flowing downstream the rack ($Q_f=Q_0-\Delta Q$);
- U = local value of the mean flow velocity along the channel;
- U_0 = mean flow velocity of the flow approaching the grid;
- $\vec{U}_g$ = velocity vector at the exit of the slit between two adjacent bars;
- U_{gn} = component normal to the rack of $\vec{U}_g$;
- W = channel width;
- x = longitudinal rack axis, with origin at the beginning of the rack;
- Y = hydraulic head;
- z = vertical (upward) coordinate, with origin at the beginning of the rack;
- z_b = bottom elevation above a horizontal datum;
- α = angle which $\vec{U}_g$ forms with the longitudinal rack axis x;
- ΔE = energy loss for unit weight of fluid experienced along a given streamline;
- ΔQ = water discharge diverted through the rack;
- Δz = difference in height experienced along the streamline;
- ω = void ratio (i.e., ratio of the rack opening area to the total area);
- ρ = water density; and
- θ = angle which the rack axis x forms with the horizontal.

References

Bouvard, M. (1953). "Debit d'une grille par en dessous (Discharge passing through a bottom grid." *Houille Blanche*, 3, 290–291.

Bouvard, M. (1992). "Mobile barrages and intakes on sediment transporting rivers." *IAHR Monograph*, Balkema, Rotterdam, The Netherlands.

Brunella, S., Hager, W. H., and Minor, H.-E. (2003). "Hydraulics of bottom rack intake." *J. Hydraul. Eng.*, 129(1), 2–10.

Davis, A. C., Jacob, R. P., and Ellett, B. G. S. (1999). "Estimating trajectory of free overfall nappe." *J. Hydraul. Eng.*, 125(1), 79–82.

De Marchi, G. (1947). "Profili longitudinali della superficie libera delle correnti permanenti lineari con portata progressivamente crescente e progressivamente decrescente entro canali a sezione costante." *Ric. Sci.* (in Italian).

Ferro, V. (1992). "Flow measurement with rectangular free overfall." *J. Irrig. Drain. Eng.*, 118(6), 956–964.

Garot, F. (1939). "De Watervang met liggend rooster." *Ing. Ned. Indie*, 7.

Hager, W. H. (1983). "Hydraulics of plane free overfall." *J. Hydraul. Eng.*, 109(12), 1683–1697.

Henderson, F. M. N. (1966). *Open channel flow*, MacMillan, New York.

Khan, A. A., and Steffler, P. M. (1996). "Modeling overfalls using vertically averaged and moment equations." *J. Hydraul. Eng.*, 122(7), 397–402.

Kuntzmann, J., and Bouvard, M. (1954). "Etudes teoretique des grilles de prises d'eau du type 'En-Dessous' (Theoretical studies of bottom type water intake grids)." *Houille Blanche*, 5, 569–574.

Marchi, E. (1993). "On the free overfall." *J. Hydraul. Res.*, 31(6), 777–790.

Mizuyama, T., and Mizuno, H. (1994). "Behavior of debris flow at control structures." *Proc., IAHR Int. Workshop on Floods and Inundations Related to Large Earth Movements*, C2.1–C2.12.

Mostkow, M. (1957). "Sur le calcul des grilles de prise d'eau (Theoretical study of bottom type water intake)." *Houille Blanche*, 4, 570–580.

Nasser, M. S., Venkataraman, P., and Ramamurthy, A. S. (1980). "Flow in channel with a slot in the bed." *J. Hydraul. Res.*, 18(4), 359–367.

Noseda, G. (1955). "Operation and design of bottom intake racks." *Proc., VI General Meeting IAHR*, Vol. 3, The Hague, C17-1-C17-11.

Noseda, G. (1956a). "Correnti permanenti con portata progressivamente decrescente, defluenti su griglie di fondo." *Energ. Elettr.*, 1, 41–51 (in Italian).

Noseda, G. (1956b). "Correnti permanenti con portata progressivamente decrescente, defluenti su griglie di fondo." *Energ. Elettr.*, 6, 565–581 (in Italian).

Oliveto, G., Biggiero, V., and Hager, W. (1997). "Bottom outlet for sewers." *J. Irrig. Drain. Eng.*, 123(4), 246–252.

Orth, J., Chardonnet, E., and Meynardi, G. (1954). "Etude de grilles pour prises d'eau du type 'en-dessous' (Study of bottom type water intake grids)." *Houille Blanche*, 3, 343–351.

Righetti, M., Rigon, R., and Lanzoni, S. (2000) "Indagine sperimentale del deflusso attraverso una griglia di fondo a barre longitudinali." *Proc., XXVII Convegno di Idraulica e Costruzioni Idrauliche*, Vol. 3, Genova, Italy, 112–119 (in Italian).

Venkataraman, P., Nasser, M. S., and Ramamurthy, A. S. (1979). "Flow behavior in power channels with bottom diversion works." *Proc., XVIII IAHR Conf.*, Vol. 4, Cagliari, Italy, 115–122.

Viparelli, C. (1963). "Dissipatori a griglia di fondo." *Energ. Elettr.*, 7, 509–519 (in Italian).

Yen, B. C., and Wenzel, H. G. (1970). "Dynamic equations for steady spatially varied flow." *J. Hydr. Div.*, 96(3), 801–814.